Linear fabrics in the Bergsdalen Nappes, southwest Norway: implications for deformation history and fold development

HAAKON FOSSEN

Fossen, H.: Linear fabrics in the Bergsdalen Nappes, southwest Norway: implications for deformation history and fold development. *Norsk Geologisk Tidsskrift*, Vol. 73, pp. 95–108. Oslo 1993. ISSN 0029-196X.

Linear structures in the Bergsdalen Nappes fall into two temporally distinct categories. The most pronounced linear set formed during large-scale Caledonian thrusting of the overlying Jotun Nappe and other nappes on to Baltoscandia. Parallelism between stretching, ribbon, mineral and intersection lineations supports previous interpretations of a close correlation between the trend of this lineation and the displacement direction in this area. A simple model of combined thrusting and horizontal pure shear with maximum extension in the flow direction is suggested, which explains the parallelism between fold axes and lineations, as well as the predominantly constrictional strain. The lineation pattern formed during thrusting indicates an overall east-southeast displacement vector, but local deviations between the different sheets and between the Bergsdalen Nappes and the Western Gneiss Region may reflect slip partitioning in addition to later reworking by extensional reversed movement of the overlying Jotun Nappe. A less pervasive set of previously neglected linear structures in the Bergsdalen Nappes marks this post-orogenic reversed movement with a top-to-the-WNW sense of shear.

Haakon Fossen, Department of Geology and Geophysics, University of Minnesota, Minneapolis, MN 55455, USA; Present address: Statoil, RGF, 5020 Bergen, Norway.

The role of lineations in orogens has been a major field of interest for about a century. In particular, there have been major discussions as to whether lineations form parallel to the principal movement direction in orogens (e.g. Sander 1930; Cloos 1946; Anderson 1948; Kvale 1953; Hobbs et al. 1976; Lin & Williams 1992). Although this issue has not been solved on a general basis, it is clear that different types of lineations may form at various angles to the transport direction, depending on factors such as the type and intensity of finite strain, strain history, deformation mechanisms, lithology, metamorphic processes and P–T conditions. Hence transverse, longitudinal, and oblique lineations have all been described from ductilely deformed rocks (Lindström 1961; Hudleston 1977; Mattauer et al. 1981; Lisle 1984; Burg et al. 1987; Dennis & Secor 1990). Kvale (1948, 1953), among others, strongly advocated the viewpoint that lineations form parallel to the tectonic transport direction (a-lineations), based on his work in the Bergsdalen Nappes, southwest Norway. However, due to the restricted understanding of shear-zone structures and mylonites in the 1940s and 1950s, Kvale was not able to distinguish between linear structures that formed during two fundamentally different deformation events in the area, and so considered all structures to be related to Caledonian thrusting. The present study provides a discussion of the various linear structures encountered in the Bergsdalen Nappes and the relationship between lineations and fold hinges in general in the light of the recent progress in understanding structural development in the ductile regime.

The Bergsdalen Nappes

The Bergsdalen Nappes (Fig. 1) are kilometer-thick slices of Precambrian rocks which originally were part of Baltoscandia, but were detached from the basement and became significantly involved in Caledonian deformation and metamorphism. They form a series of thin, lensoid nappes, each enwrapped by dark phyllite and mica schist, and 'sandwiched' between Baltoscandia (basement) and

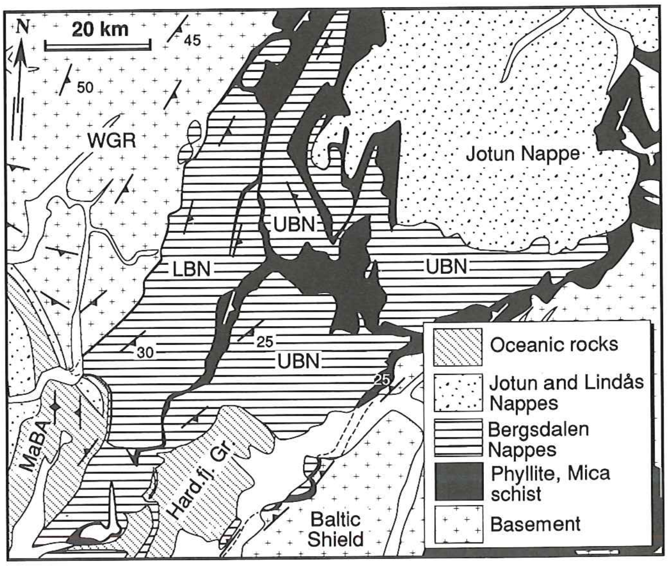

WGR=Western Gneiss Region, LBN=Lower Bergsdalen Nappe, UBN=Upper Bergsdalen Nappe, MaBA=Major Bergen Arc, Hard.fj. Gr. = Hardangerfjord Group

Fig. 1. Simplified geological map of the Bergsdalen Nappes and surrounding units. Modified from Kvale (1960).

the overlying Jotun Nappe Complex. The phyllite and mica schist are considered to be, at least partly, Lower Paleozoic in age, and to be part of the continuous belt of strongly sheared phyllitic rocks that underlie the Caledonian nappes in southern Norway.

The Bergsdalen Nappes may be separated into two major units, an upper (UBN) and a lower nappe (LBN) separated by strongly sheared phyllite. Both consist of a variety of altered sedimentary, volcanic and igneous rocks (Kvale 1946). Quartzite, quartz schists and minor mica schists and conglomerates are intercalated with metavolcanic rocks ranging from metabasalt (amphibolite) through to metarhyolite. This supracrustal sequence bears similarities to the Proterozoic Telemark Group (Kvale 1946), which is an infolded and integral part of the autochthonous Baltic shield to the southeast (Dons 1960). The supracrustal rocks were intruded by gabbroic bodies and mafic dikes (amphibolites), and finally by a number of granites and related dikes. Several of the granitic bodies and the rhyolite have been dated by the Rb–Sr whole-rock method to give ages in the interval 1274 ± 48 Ma through to 971 ± 71 Ma (Pringle et al. 1975; Gray 1978).

Detailed fieldwork (Fossen 1993) has failed to demonstrate any significant Precambrian deformation in the supracrustal rocks of the Bergsdalen Nappes: none of the numerous dikes have been found to cross-cut any earlier deformation fabric. However, they do cross-cut primary sedimentary structures in low-strain areas. Discrete sets of en échelon sigmoidal quartz veins are the only deformation structures demonstrably being cross-cut by granitic dikes. The penetrative linear and planar fabrics that dominate and characterize the Bergsdalen Nappes affect all lithologies in the region, including the phyllites and mica schists between the nappes. Hence, being predated by the Sveconorwegian granitic intrusives, the deformation fabrics are most likely to be Lower Paleozoic, as inferred by Kvale (1948).

Detailed kinematic analysis of rocks in the Bergsdalen Nappes (Fossen 1992a, b, 1993) has recently unravelled two major and distinct Paleozoic kinematic events. The first event (D1) involved top-to-the-E or SE shear deformation and is related to the main Caledonian nappe translation in Silurian (?) times. The second event (D2) was basically a reversal of the D1 movement to form asymmetric shear zone fabrics that indicate top-to-the-WNW transport. Both events involved extensive synkinematic recrystallization under middle to uppermost greenschist facies conditions, and their heterogeneous nature has resulted in areas of low D2 and high D1 strains and vice versa. Also, both events produced lineations, hence the present lineation pattern is a combination of lineations formed during D1 and D2, albeit with the D1 fabric being the strongest.

Lineations related to Caledonian thrusting (D1)

A variety of lineations formed during the thrusting (D1) event. These are best studied in areas of weak or no D2

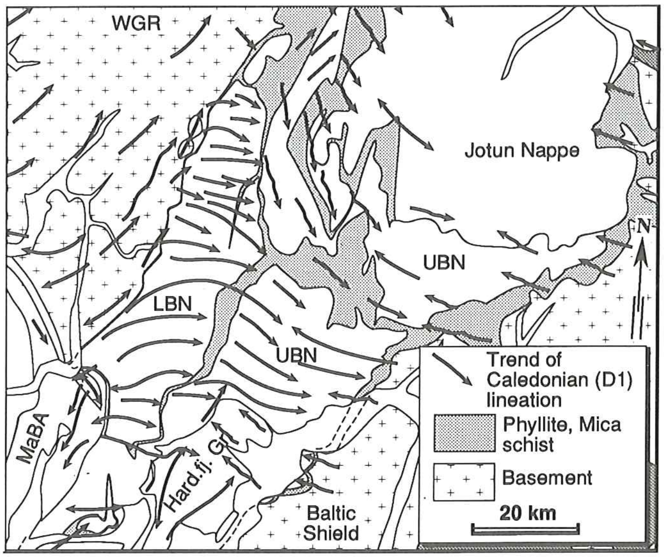

Fig. 2. Trend of D1 lineations related to top-to-the-(S)E thrusting in the area covered by Fig. 1.

reworking, but they can be recognized in any part of the Bergsdalen Nappes (Fig. 2), and may in many places be traced continuously into the overlying Jotun Nappe and the underlying Western Gneiss Complex.

Ribbon and stretching lineations in sheared igneous rocks

Ribbon lineations are common in large portions of the Bergsdalen Nappes, particularly in deformed granitoids and metarhyolites. They have a general E–W to SE–NW trend (Fig. 3a), and variations in trend are generally smooth. This lineation is defined by millimeter to centimeter-wide white and/or reddish ribbons or lenticular aggregates of quartz and feldspar enveloped by relatively thinner, more fine-grained and completely recrystallized feldspar–quartz–mica layers. The quartz–feldspar ribbons are typically long aggregates or bands in sections parallel to the lineation and normal to the foliation. In sections perpendicular to lineation, the same aggregates are considerably shorter, locally near equidimensional. However, gradations from this characteristic L-fabric to LS or S-fabrics occur.

Feldspar porphyroclasts (deformed phenocrysts) are moderately deformed by crystal-plastic deformation, and small tails of recrystallized feldspar grains occur. In mylonitic granitoids, feldspar porphyroclasts more commonly 'break up' into aggregates consisting of cores of the original feldspar mantled by finer grained, dynamically recrystallized feldspar grains. Several porphyroclasts continue laterally into millimeter-thick bands of nearly pure quartz and small amounts of sericite. Such thin bands of dynamically recrystallized quartz are a major constituent of the quartz–feldspar ribbons defining the ribbon lineation, and probably represent sinks of silica transferred from the now more mica-rich layers (L-layers) by diffusion (cf. Robin 1979). Hence, a variety of deformation mechanisms and processes (e.g. Kerrich

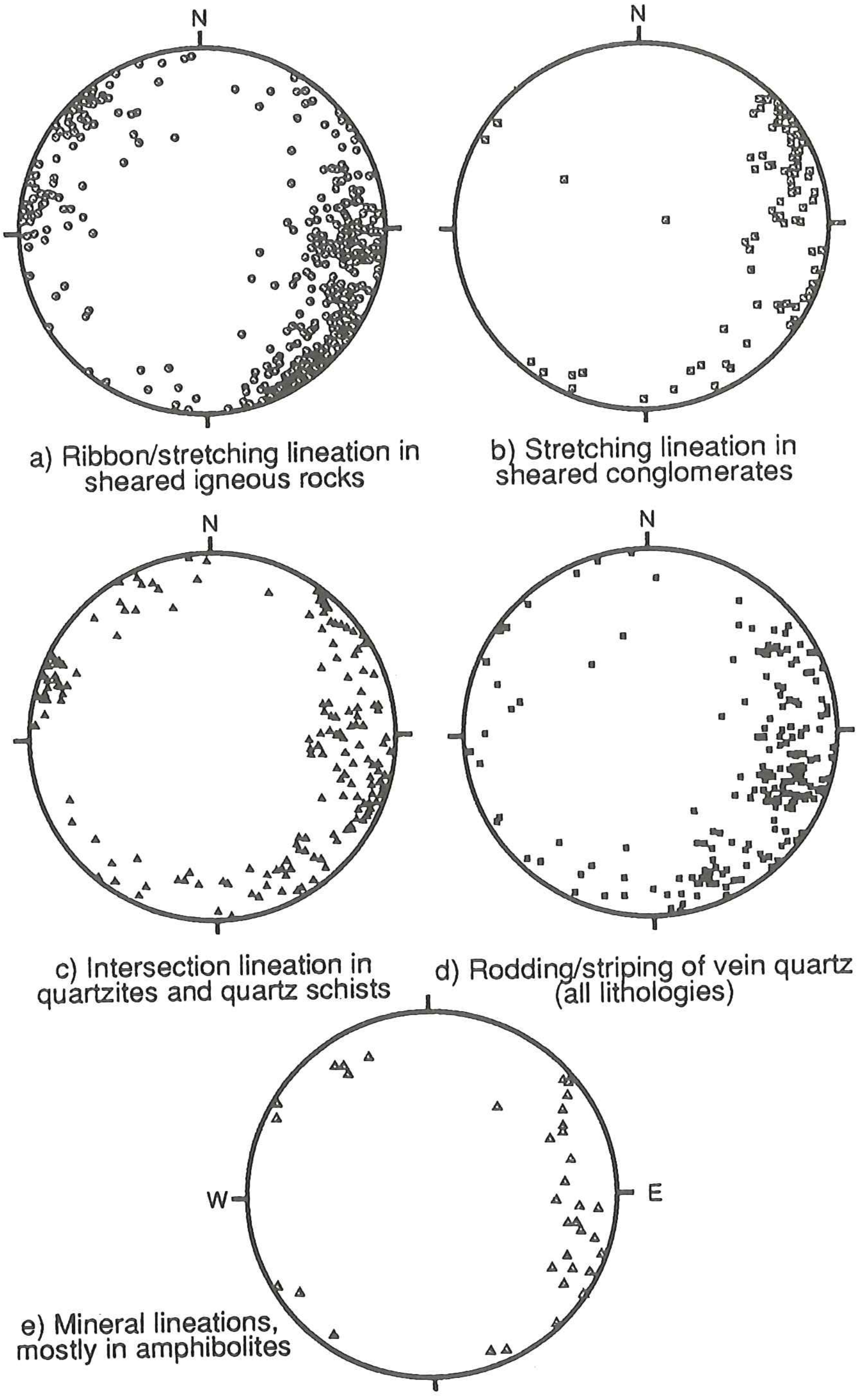

Fig. 3. Stereograms of D1 lineations from the Bergsdalen Nappes (equal-area lower hemisphere projection).

& Allison 1978, Shedl & Pluijm 1988), including metamorphic differentiation (solution transfer), recrystallization, and grain-size reduction of porphyroclasts (cf. Vernon 1974) contributed to the development of the ribbon lineation.

As the formation of the ribbons involves stretching of minerals and mineral aggregates by ductile and brittle processes, the resulting lineation is a stretching lineation where the long axes of the stretched aggregates define the stretching or shape fabric lineation. This lineation will not necessarily be parallel to the local long axis (λ_1) of the strain ellipse, owing to the contrasting mechanical properties of the various minerals, and to grain-scale strain partitioning. However, for moderate and high strains the difference may be considered small or negligible. There is thus a close relationship between this type of stretching lineation and that seen in deformed conglomerates (below), as indicated from previous studies of similar rocks (Wilson 1975; McLelland 1984).

Stretching lineation in metasediments

A most spectacular and striking lineation in the area is defined by the long axis of stretched pebbles in deformed conglomerates. Conglomerates occur in both the Upper and Lower Bergsdalen Nappes, but the conglomerates of the UBN have pebbles of granitoids, vein quartz, and quartzite which show relatively high competency contrast to the quartz–mica schist matrix. Pebbles in the UBN were also folded, locally multiply, after the main part of the D1 deformation, and are not very well suited for quantitative strain evaluation. The shapes of most pebbles seem, however, to be of the prolate type, and the maximum elongation direction is typically parallel to other, nearby lineations. In contrast, the conglomerates found in the Lower Bergsdalen nappe have vein quartz and quartzite pebbles in a quartzitic matrix. These conglomerates possess pebbles with prolate shapes with very few exceptions, as indicated by Kvale (1948). The pronounced prolate pebble shapes are easily visible in the field, and are confirmed by strain measurements where such could be obtained (Fig. 4). The trend of the maximum finite stretching direction (λ_1) recorded in the conglomerates is indicated in Fig. 3b. Biasing of the λ_1 trend about ENE (Fig. 3b) rather than the more common ESE trend seen in Fig. 3a is caused by the restricted extent and distribution of conglomerates relative to the regional variation of the general lineation trend.

At a few localities the white quartzite possesses an angular network of darker, gray-colored grains (Fig. 5). The shape of this network is quite regular in sections normal to the lineation, but strongly elongated in sections parallel to the lineation and perpendicular to the foliation. It seems likely that the network structure originated by fracturing of the sandstone during diagenesis accompanied by fluid flow and associated decoloration along the fractures. The network was then stretched during D1 to form this special kind of stretching lineation.

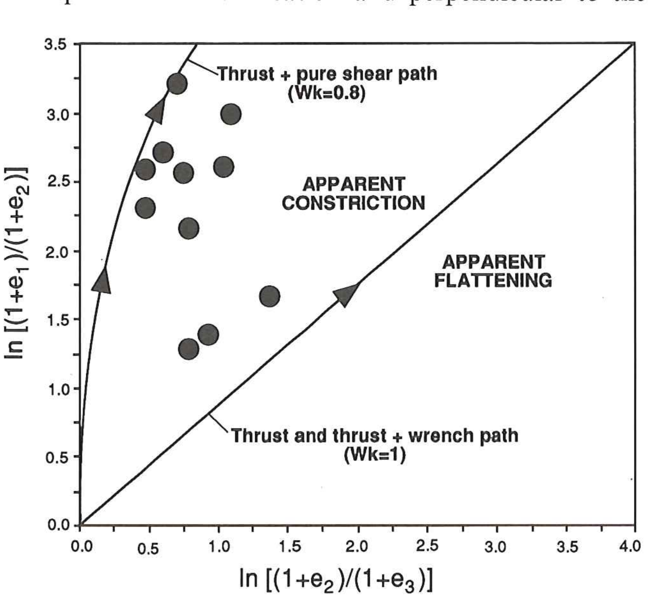

Fig. 4. Strain data from deformed quartzite conglomerates in the LBN plotted on a logarithmic Flinn diagram together with paths resulting from the strain models discussed in the text (see Fig. 10).

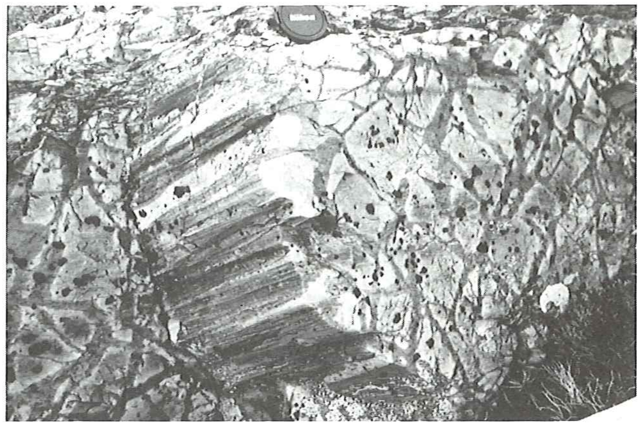

Fig. 5. Deformed network of darker, grayish decolored grains, forming a stretching lineation in the LBN. Note the shape of the fragment, indicating constrictional strain. Lower Bergsdalen Nappe near Alexander Grieg-hytten, Bergsdalen (UTM LN344083).

Intersection lineation

The intersection of compositional layering in metavolcanic rocks or bedding in metasediments with the penetrative S1 foliation gives rise to a lineation (Fig. 3c). This intersection lineation is the dominating lineation in quartzites of the LBN (Fig. 6). Its trend closely compares to the stretching lineation in interbedded conglomerates and to the ribbon lineation in cross-cutting granites.

A similar lineation is developed in more strongly deformed, micaceous lithologies, e.g. quartz-mica schists and metadacite, where the S1 foliation is refolded during progressive deformation. An intersection lineation is then defined by the intersection between the folded and the new foliation.

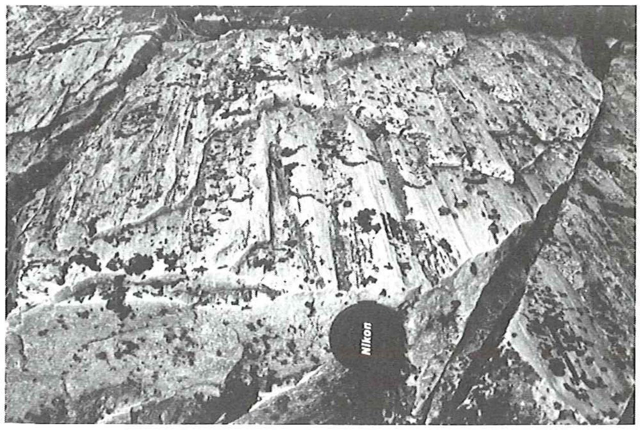

Fig. 6. Typical intersection lineation between layering in quartzite and S1. Lower Bergsdalen Nappe near Alexander Grieg-hytten, Bergsdalen (UTM LN395170).

Other lineations

The lineations in some of the intensely sheared quartzites and quartz schists appear as a fine 'corrugation' on fracture surfaces (Fig. 7). This lineation is different from stretching lineations in that the quartz grains are generally only weakly elongated and not necessarily elongated in a direction parallel to the lineation.

A similar and very characteristic lineation in the region is found at the interface between bands of sheared, pure vein quartz and the host rock, or along micaceous layers between isoclinally folded and sheared quartz bands (Fig. 3d). The lineation may partly be controlled by the viscosity contrast between the pure quartz bands and the host rock, i.e. akin to the formation of fold mullions (Hobbs et al. 1976, pp. 276–278).

Some of the strongly sheared, impure quartzites show a characteristic rodding lineation, where rods of fairly pure quartzite occur in a more mica-rich matrix, i.e. resembling strongly stretched conglomerates (Fig. 8). It is assumed that this type of lineation formed as a combination of folding and constrictional deformation of a layered series of alternating quartzite and quartz–mica schist.

Mineral lineations (Fig. 3e), other than those defined by elongated feldspar and quartz (above), are defined by aligned amphiboles in the amphibolites and elongated and recrystallized micas. These lineations are generally parallel to the lineations mentioned above, although local deviations have been observed in some amphibolites.

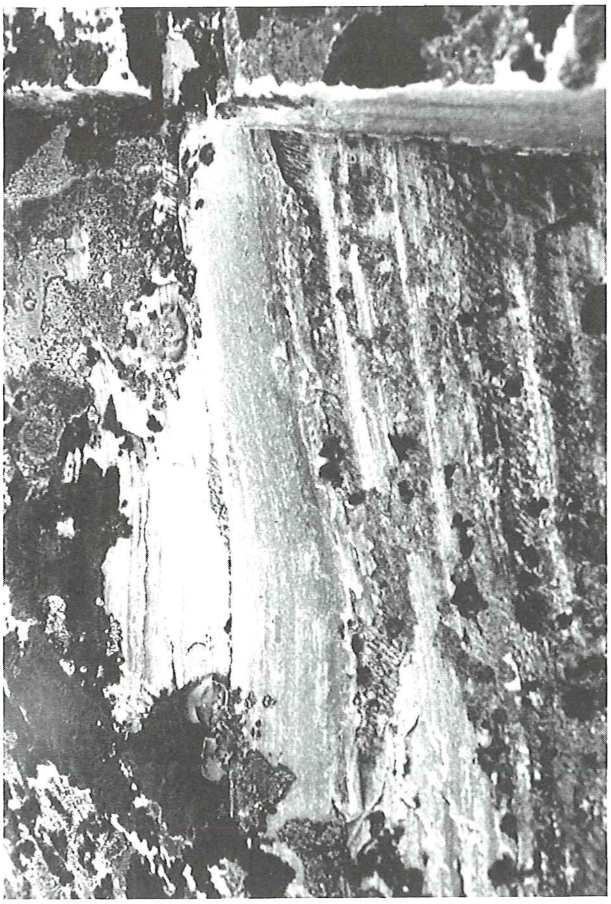

Fig. 7. Close-up of quartzite surface, showing the strong and characteristic 'striping' of the D1 lineation. A weak D2 crenulation lineation is locally developed oblique to the D1 lineation. Northern side of Bergsdalen (UTM LN414186).

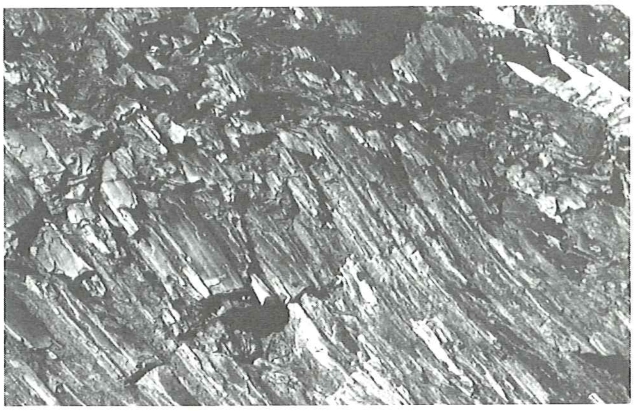

Fig. 8. Lineation in rodded quartz schist, resembling stretched conglomerates in the constrictional field. Upper Bergsdalen Nappe south of Hamlagrøvatnet (UTM LN417075).

Crenulation lineations are associated with and parallel to the intersection lineations discussed above, and with fold hinges discussed below. However, a crenulation lineation which formed at a very late stage during D1 in parts of the UBN has a NE trend oblique to the general linear pattern (Fossen 1993). This crenulation lineation, which is interpreted as a late pulse of the D1 deformation, is not included in the discussions below.

Fold hinges

The most distinct folds in the Bergsdalen Nappes developed during the post-Caledonian backward movement of the nappes as discussed below. However, small-scale folds, which developed along with the D1 lineations discussed above, do occur. These folds are refolded by the later, NW-verging D2 folds described below. Characteristic of the D1 (thrusting) deformation is the formation of folds with hinges mostly parallel or subparallel to the lineation (Fig. 9). This feature has been described from several ductile high-strain zones throughout the world (e.g. Bryant & Reed 1969; Rhodes & Gayer 1977; Bell 1978; Williams 1978; Kirschner & Teyssier 1992) and it represents a classical problem to which a simple, general solution may or may not exist. However, several models can be applied to produce parallel fold hinges and lineations. They can be grouped into those that do and do not involve rotation of fold hinges, as discussed in the next section.

Rotation of hinges by simple shear

The most popular model involves the formation of fold hinges close to (but not exactly parallel to) the λ_2-axis of the strain ellipsoid in simple shear and their progressive rotation towards the λ_1-axis and the lineation by increas-

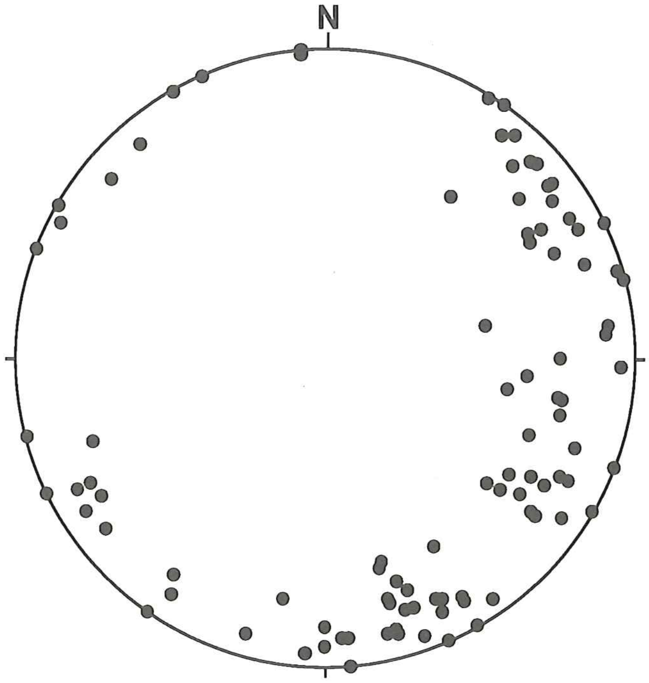

Fig. 9. Orientation of F1 fold axes in the Bergsdalen Nappes. A late family of SE-verging D1 cross-folds, which is restricted to the southern part of the UBN, is not included. Equal-area lower hemisphere projection. Compare with Fig. 3.

ing shear strain (Lindström 1961; Bryant & Reed 1969; Roberts & Sanderson 1973; Sanderson 1973; Escher & Watterson 1974; Rhodes & Gayer 1977; Bell 1978; Williams 1978; Cobbold & Quinquis 1980; Vollmer 1988). A major problem with this model is that for simple shear deformation, fairly high shear strains are required to rotate folds into close parallelism with the lineation (Skjernaa 1980). It has, however, been applied successfully to some regions of demonstrably strongly non-cylindrical (sheath) folds (Henderson 1981; Lacassin & Mattauer 1985; Vollmer 1988).

Rotation by non-simple shear

Ramsay & Graham (1970) showed that the only compatible strain within a planar, ductile shear zone with undeformed or homogeneously deformed wall rock is simple shear with or without dilatation. However, strain analyses reported from natural shear zones indicate that deviation from simple shear strains is the rule rather than the exception, owing to strain partitioning within shear zones, curved shear zone boundaries, mechanical instabilities, spatial variations in strain rates etc. The effect of various types of deformation on fold-axis rotation therefore should be considered in this discussion. However, for the sake of simplicity and clarity, the rotational models considered in this paper assume steady-state deformation, i.e. fixed instantaneous stretching axes and constant kinematic vorticity number (Means et al. 1980) throughout the deformation.

Lateral differential movements within horizontal shear zones (e.g. in thrust zones) create deformation that can

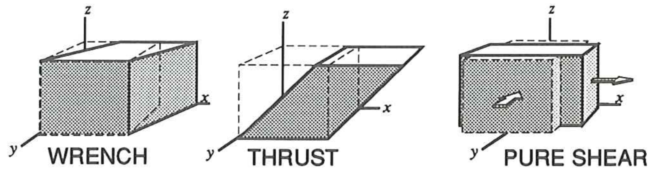

Fig. 10. The three deformations that are combined simultaneously to form the three strain models considered in the text, i.e. thrusting, simultaneous thrusting and wrenching, and simultaneous thrusting and pure shear.

be resolved into a horizontal simple shear ('thrust' in Fig. 10) caused by an overriding thrust sheet (in this case the Jotun Nappe), and a vertical simple shear ('wrench' in Fig. 10) (cf. Coward & Potts 1983, Ridley 1986, Kirschner & Teyssier 1992). For the simplest case the intersection between these two planes would be parallel to the displacement direction of the thrust sheet. Coward & Potts (1983) argued that this mechanism provides more rapid rotation of fold hinges towards the lineation than thrusting alone. Their main assumptions were that the layering to be folded is horizontal, that the axial planes of the folds are parallel to the $\lambda_1-\lambda_2$ plane of the finite strain ellipse, and that folds initiate parallel to the maximum resolved stretching direction in the plane of layering.

There is an infinite number of other strain models that may be applied, depending on the information that can be gathered in the field about the strain and strain history in a particular area. However, a simple model which provides efficient rotation of fold hinges is a simultaneous combination of thrusting ('thrust', Fig. 10) and a horizontal pure shear (compression along λ_2 and extension along the slip direction, 'pure shear' in Fig. 10). This model has also been chosen because it produces strains comparable with those observed in the Bergsdalen Nappes (see below).

Evaluation of three rotational models

A general evaluation of the different models, i.e. thrust alone, thrust + wrench, and thrust + pure shear (Fig. 10) is not available from the present literature, and a series of three-dimensional computer simulations have therefore been carried out. It is assumed that the folds behave passively, i.e. that their hinges rotate as passive line markers, and that deformation is homogeneous (cf. Flinn 1962). These are simplifications, since the deformation clearly is heterogeneous and several of the fold structures involve layers of varying competency. However, the approximation that strain is homogeneous on the scale of minor folds is reasonable, and the treatment of fold axes, being mathematical rather than physical lines, as passive lines is probably acceptable in the present context. Folds commonly initiate with a preferred orientation which depends on factors such as the type and orientation of the incremental strain, rheological factors and the orientation of the layering relative to the instantaneous stretching axes. For a general discussion, it is useful to study an initially random distribution of fold axes, in which case the history of any initial orientation can be recognized.

One thousand randomly distributed fold axes were deformed using the methods described by March (1932), Flinn (1979) and Fossen & Tikoff (1993) (see Appendix). The random distribution was deformed to five different states of finite strain (Fig. 11). Comparing three-dimensional strains is not straightforward. The best and most widely used measure of general strain is probably

$$\bar{\varepsilon}_s = \frac{\sqrt{3}}{2}\gamma_0$$

where γ_0 is the natural octahedral unit shear (cf. Hsu 1966; Hossack 1968). The strain ($\bar{\varepsilon}_s$-value) in each of the five stages in Fig. 11 corresponds to the strain produced by a simple shear of $\gamma = 1$, 2, 3, 5 and 10, respectively.

The results show that for thrusting alone (Fig. 11A) a high concentration of fold axes parallel to the lineation (λ_1) is achieved after a shear strain of ca. 10 ($\bar{\varepsilon}_s = 3.27$). However, the rotation is much slower for fold axes that were initially close to the shear plane (primitive circle) than for more steeply plunging hinges. The concentration along the shear plane in Fig. 11A (thrusting) is the result of these differential rotation velocities.

Rotation of hinges for a combined thrust and wrench (Fig. 11B) shows a rate of clustering similar to that of thrusting. The degree of clustering should ideally have been exactly the same, since both are simple shear deformations, but slight differences occur due to the initial random distribution and to the contouring procedure (Fig. 12). Again, axes close to the shear plane rotate slowest, giving rise to the preferred orientation along a great circle which by increasing finite strain approximates the resultant shear plane (045/45 in present case where thrust and wrench components are of equal magnitude). However, the trend of the lineation deviates from the slip direction (X) in this case, except for high strain values.

A simultaneous combination of thrusting and pure shear (Fig. 11C) provides more effective rotation of fold hinges. In this case, there is no significant difference in rate of rotation between hinges of different initial orientation, even though the component of pure shear relative to thrusting is relatively low (the kinematic vorticity number $W_k = 0.8$). (In two dimensions, W_k can be looked at as a measure of the relative amount of pure and simple shear involved in a deformation, where $W_k = 1$ for simple shear, and $W_k = 0$ for pure shear.) For a stronger pure shear influence (lower W_k), even higher concentration would develop for a certain amount of strain.

Another interesting fact that emerges from these simulations is that the maximum concentration of rotated hinges is always very close to the principal extension direction (λ_1) (Fig. 11). Hence, starting with a random distribution of fold axes or other lineations, only the variation in density of fold axes around λ_1 is significant for the different types and magnitudes of strain.

In order to obtain a better impression of the rotation of individual lines, a set of hinge orientations (135/0, 135/05, 135/45, 090/0, 090/05, 090/45, 045/0, 045/05, 045/45, and 000/90) was deformed progressively according to the three different strain models described above. Previous investigators have mostly been concerned with the angle between hinges and the shear direction (X in this paper). However, a more realistic approach is to consider the angle between the hinge and λ_1, since the measured lineations in general, and in particular in the Bergsdalen Nappes, represent or are subparallel to the finite stretching direction (Kirschner & Teyssier 1992). The general particle flow patterns for the three cases are shown in Fig. 13. Each arrow represents the rotation caused by a strain of $\bar{\varepsilon}_s = 0.176$, and the length of the arrows thus indicates the local rate of hinge rotation.

The change in angle between fold hinges and λ_1 (Fig. 14) leaves the same impression as do Figs. 11 and 12, i.e. that rotation is considerably more effective for a combination of thrusting and pure shear. An interesting feature is that steep hinges rotate fast for thrusting (Figs. 13a, 14a), whereas shallowly-plunging hinges rotate more slowly. For a combined thrust and sinistral wrench (Figs 13b, 14b), hinges plunging towards the negative Y coordinate axis (towards 270) rotate fast, whereas those situated close to the inclined shear plane (045/45) rotate slower. For combined pure shear and simple shear (Figs. 13c, 14c), hinges plunging steeply towards the negative X-axis rotate fast. Due to the non-plane strain nature of this deformation, however, all hinges except those exactly parallel to X rotate to some extent. Note that a limited population of gently plunging hinges in the first and fourth quadrant take on highly curved paths as they start to rotate towards X counter to the thrust component, but soon after turn around to rotate sympathetically with the thrusting.

No rotation of fold hinges

Folds may *initiate* with hinges parallel to the lineation. In a shear regime, this generally requires non-steady state flow. For example, a strain history where thrusting occurs intermittently with local shortening (pure shear) in the horizontal plane perpendicular to the thrusting direction would generate folds with axes parallel to λ_1 (assuming that the thrusting already has formed a subhorizontal layering). The anisotropy represented by the pre-existing lineation further increases the likelihood of fold axes forming with axes parallel to λ_1 (cf. Hanmer 1979). Such a strain history may account for heterogeneities in the flow or shear zone system caused by anastomosing shear zones, anisotropic and heterogeneous rocks, differential movements, non-planar shear zone boundaries, etc. A somewhat similar model has been mentioned as a possible explanation for rodded conglomerates in the Bygdin area (Hossack 1968). Models involving a temporary component of lateral shear in a direction Y perpendicular to the thrusting direction (X) may also generate folds

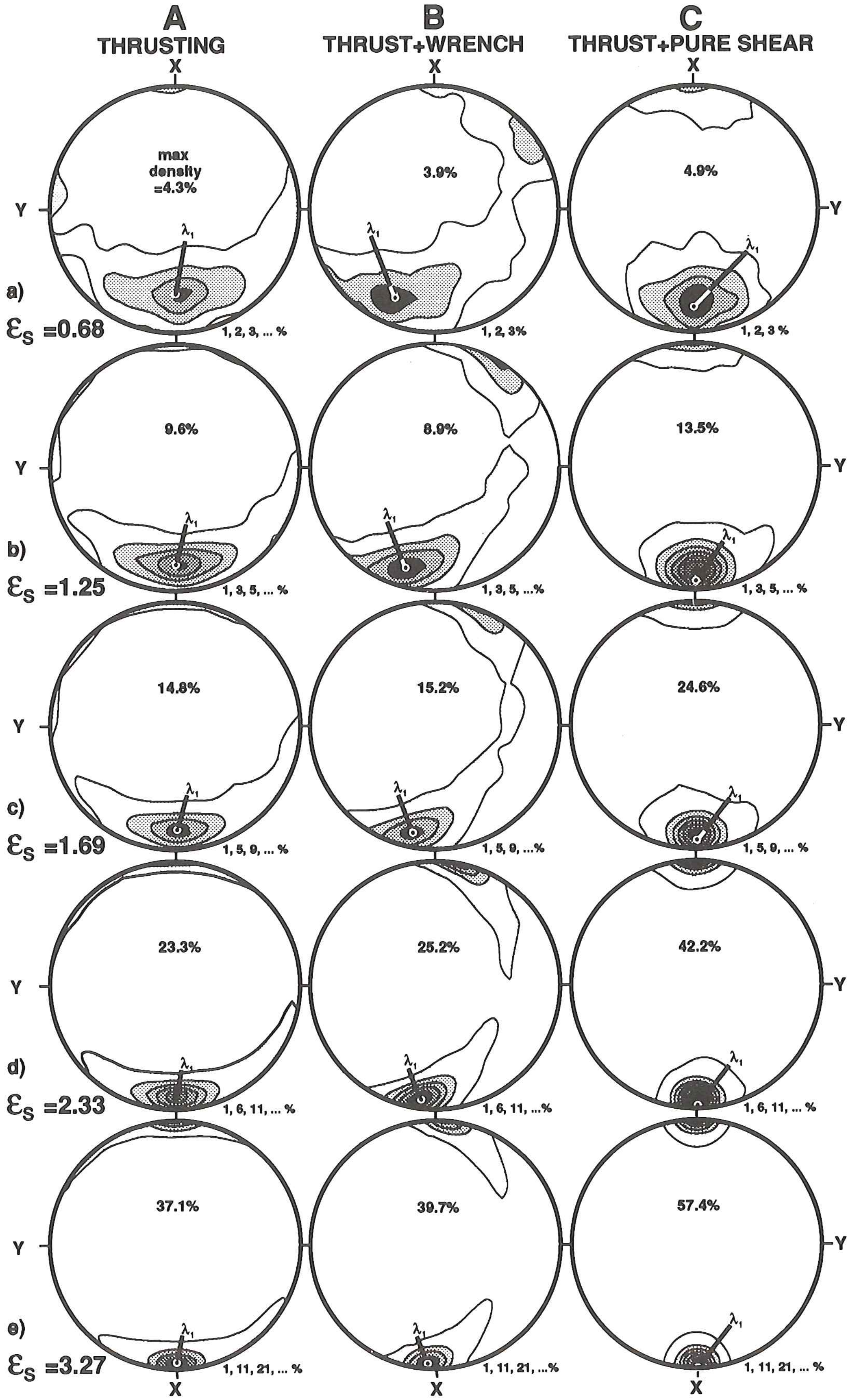

Fig. 11. Spatial distribution of 1000 initially randomly oriented fold axes deformed passively by thrusting (column A), thrusting and wrenching (equal magnitude, column B), and simultaneous thrusting and horizontal pure shear (kinematic vorticity number = 0.8, column C). The strain is constant along each row, corresponding to a shear strain of 1, 2, 3, 5 and 10 in (a), (b), (c), (d) and (e), respectively. Equal-area projection. X = shear direction. See text and Appendix.

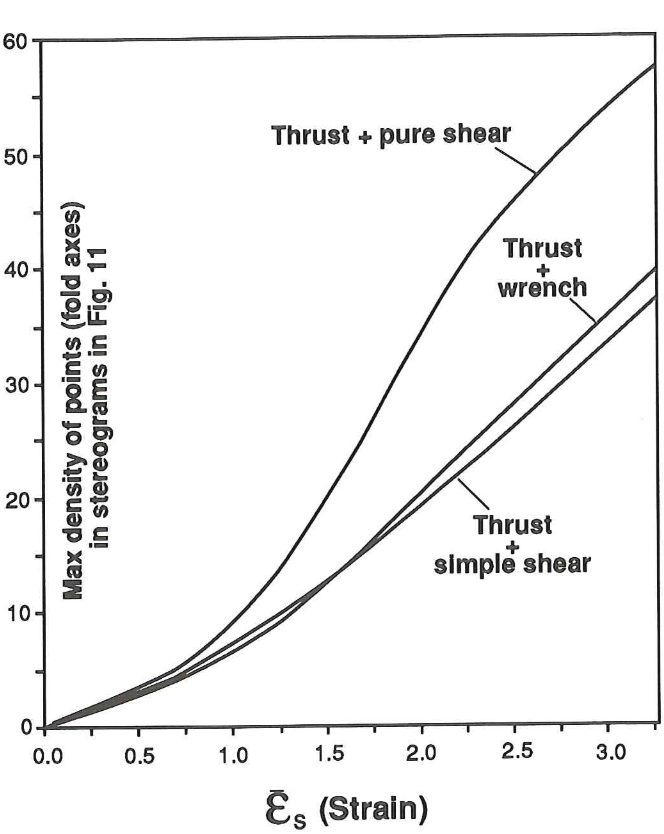

Fig. 12. Graph of variation in maximum density (%) of points (fold axes) in Fig. 11 with increasing finite strain for an initially random line-distribution deformed by thrusting, thrusting and wrenching, and simultaneous thrusting and horizontal pure shear. The latter deformation provides the fastest clustering of lines of the three models.

with hinges subparallel to X, partly because of the anisotropy represented by the pre-existing lineation (cf. Hanmer 1979). However, constrictional finite strain is only expected in the hinge region of the newly formed folds, particularly if the pre-existing fabric is of the flattening type. A possible example of this is the folded conglomerate in the Rundemanen Formation, Bergen, where the fold axis and stretching direction measured in deformed pebbles are parallel within the error of measurement (Holst & Fossen 1987; Fossen 1988), and where constrictional strains are confined to the hinge zones. However, the general strain would still be nonconstrictional, i.e. different from that observed in the Bergsdalen Nappes (Fig. 4).

A more special situation is where a pre-existing layering was vertical with strike parallel to the thrusting direction (X) at the initiation of deformation. In this case folds may be expected to initiate parallel to the fastest instantaneous stretching direction, and the lineation would evolve parallel with the folds (see also Treagus & Treagus 1981). Although the fold axis does rotate with

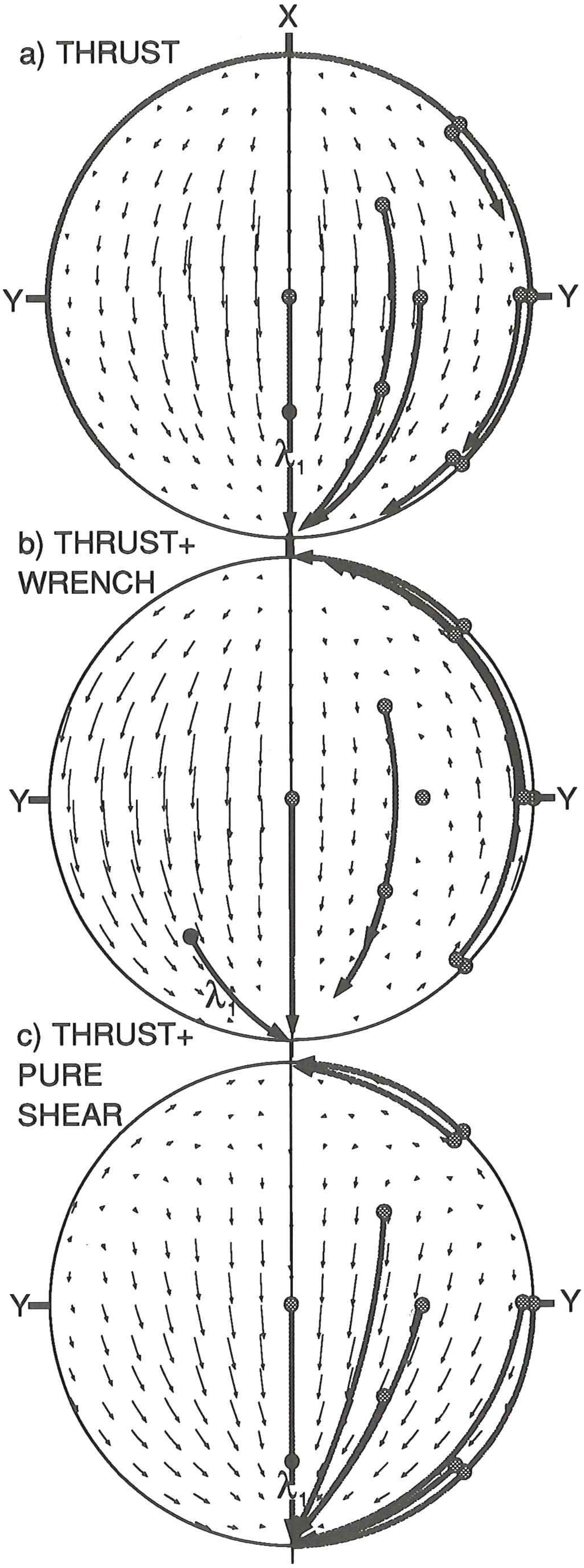

Fig. 13. Paths of line rotation for the three different deformations discussed in the text. Length of lines indicates amount of rotation for a strain magnitude of $\bar{\varepsilon}_s = 0.1763$ which, for (a) and (b), corresponds to a shear strain (γ) of 0.25. The length of lines therefore reflects the local rate of rotation. The rotation paths for ten differently oriented lines are indicated (see text for discussion).

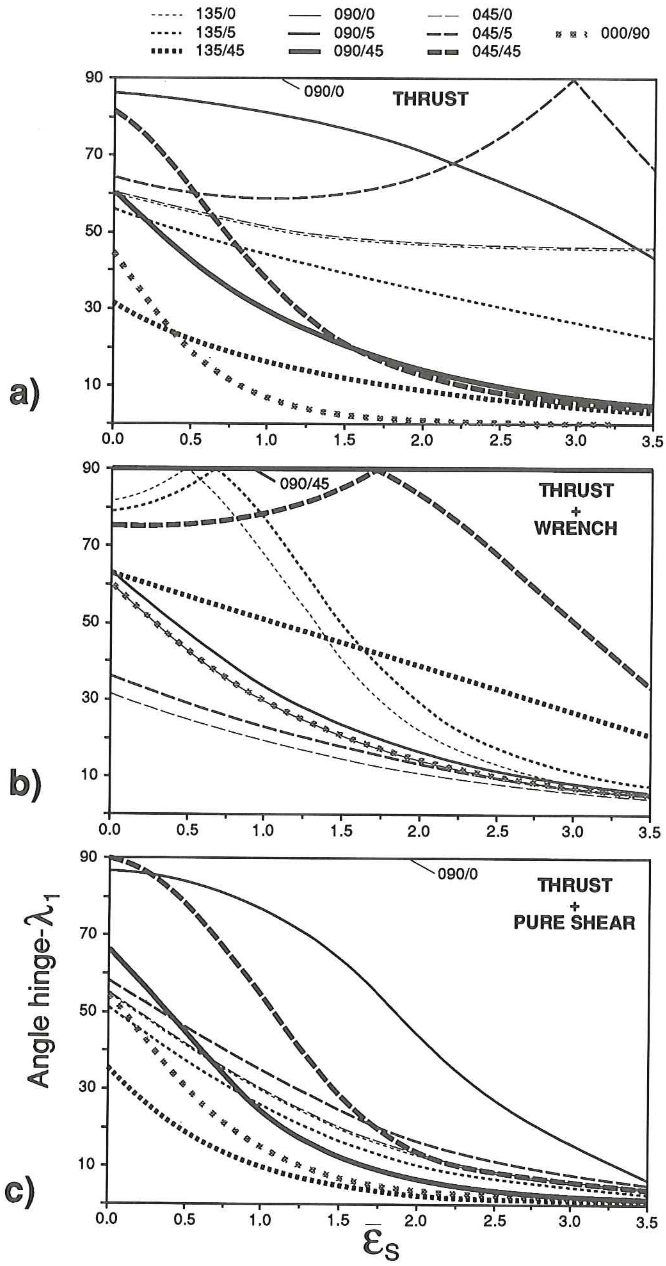

Fig. 14. Variation of the angle between the maximum elongation direction and the ten lines indicated in Fig. 13, with increasing strain. This angle decreases faster for simultaneous thrusting and pure shear (c) than for the other cases (a and b).

respect to the shear plane in this case, its rotation with respect to the lineation is modest.

Observations and discussion

F1 folds in the Bergsdalen Nappes are thought to have formed throughout the D1 deformation. They display a variety of styles and occur in all lithologies, but are most common in quartzitic rocks and deformed metavolcanics. The fold types may be grouped into (1) those deforming primary structures, (2) those deforming already foliated rocks, and (3) those deforming quartz veins. The first type is widespread in quartzites of the Lower Bergsdalen Nappe. The folded layers are Precambrian granitic dikes in the quartzite and, more commonly, sedimentary layering, in which case subsimilar fold geometries are common. Direct measurement of fold axes in the field is not everywhere possible, but the constant orientation of the intersection lineation strongly indicates lineation-parallel fold axes. Moreover, close parallelism with the local stretching lineation in low as well as high-strain regions indicates that these folds either rotated rapidly towards, or formed parallel with λ_1. Furthermore, the state of strain in the quartzite conglomerates is highly constrictional (Fig. 4), and thus not compatible with plane strain (e.g. simple shear).

Folds affecting previously foliated rocks may be subdivided into two types. One is widespread in quartz schists and foliated metavolcanics, and the structures of this type fold a somewhat older D1 foliation (Fig. 15). These folds vary from open and upright through isoclinal recumbent folds, most of which are parallel to the local stretching lineation, again indicating either non-rotating or rapidly rotating fold hinges. The second kind of foliation-deforming folds are subsimilar (class 2) folds found in mylonite zones in more massive quartzites. These folds are highly non-cylindrical and asymmetrical recumbent or overturned folds, and their axes make various angles with the local lineation. The sheath-like geometries of several of these folds indicate rotation of fold hinges towards the lineation during deformation, but as the amount of strain these folds have experienced is unknown, the rate of rotation is not known.

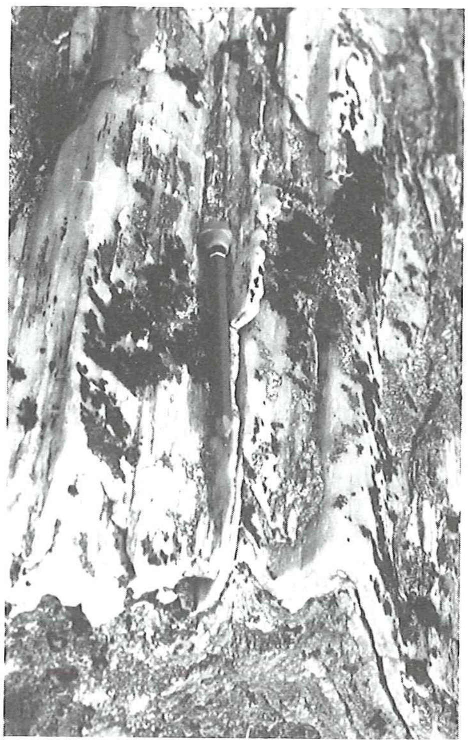

Fig. 15. Upright folds folding the foliation in a mylonitic quartz schist in UBN, with axes perfectly parallel to the lineation. South of Hamlagrøvatnet (UTM LN410095).

The last type of D1 folds, defined by folded and well lineated vein quartz, is also common throughout the region, but is generally restricted to high-strain zones and schistose, micaceous lithologies (quartz (-mica) schists, biotite-rich, mafic metavolcanics, and mica schists). Close parallelism between the lineation and the hinge line is also characteristic of these folds. The quartz veins must have rotated towards parallelism with the foliation during deformation. Provided there is no significant viscosity contrast between the quartz veins and the matrix (quartz veins in quartzite), the foliation around such veins may become folded during rotation (see Hudleston 1989). A characteristic feature of this type of fold is the apparently 'wrong' sense of displacement across the vein, a feature encountered in some of the folds in the Bergsdalen Nappes. Following Hudleston's model, a majority of these folds are expected to have initiated with their axis at a high angle to the lineation and then rotated at rates and along paths depending principally on their initial orientation and the governing strain type.

Neither thrusting nor a combination of thrusting and wrenching are compatible with the observed finite strain in the deformed conglomerates in the LBN. However, the model involving simultaneous horizontal pure shear and thrusting implies strain paths within the constrictional regime, and the path resulting from the example above ($W_k = 0.8$) is indicated in Fig. 4. As a general model, a combination of pure shear and thrusting is thus preferable.

Lineations related to reversed movement (extension)

A fairly penetrative, regional linear fabric was established during D1. In general, the sense of vorticity was reversed during D2, and the D1 fabrics were variably reworked. In zones of moderate to high D2 strain, the pre-existing D1 linear fabric was modified by renewed dynamic recrystallization. Completely new D2 lineations formed in areas of low D1 strain and high D2 strain. In many cases it is, however, hard to distinguish new D2 lineations from reworked D1 lineations, particularly because most D2 lineations are very similar to the D1 lineations described above. This is particularly true for ribbon and mineral lineations formed in meta-igneous rocks. The D2 data presented here has therefore been selected from rocks where the intensity of the D2 fabrics is high enough to avoid possible confusion with D1 lineations.

D2 mineral and stretching lineations

The D2 mineral and stretching lineation is best developed in mica-bearing rocks of the Bergsdalen Nappes, e.g. in metadacites or mica gneisses, and particularly in the phyllites and mica schists between the Bergsdalen Nappes. The micaceous rocks typically contain rodded quartz, which in part is a D1 lineation that has been reworked by rotation and recrystallization during D2. The D2 stretching lineations occur locally in deformed magmatic rocks, and are found together with fibre lineations in micaceous rocks. Lineations in micaceous lithologies are frequently associated with shear bands or S–C structures indicating a top-to-the-northwest sense of shear, and lineations developed in these shear bands are taken to be of D2 age. Conspicuous D2 lineations in the micaceous rocks (Fig. 16a) and in quarzofeldspathic lithologies (Fig. 16b) quite uniformly indicate a shear direction about 290–300 (WNW) during D2. This is consistent with the direction perpendicular to the trend of the S–C intersection line of S–C structures formed during D2 (Fig. 16c).

D2 fold hinges

Whereas parallelism between fold hinges and other lineations is characteristic of the D1 deformation, this is not

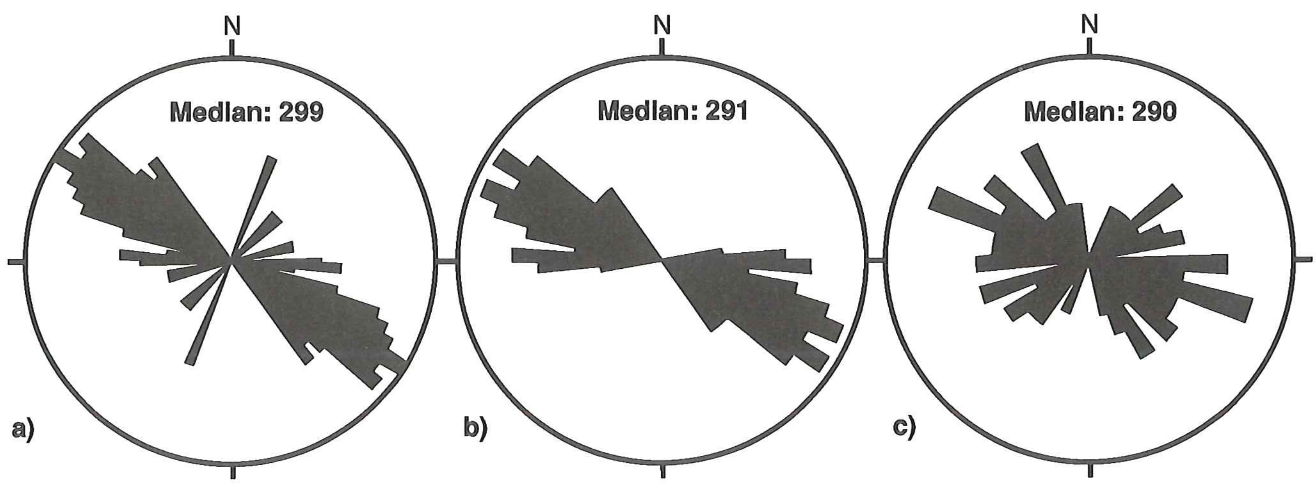

Fig. 16. Reversed movement (D2) shear direction as indicated from (a) D2 lineations in micaceous rocks (phyllites, mica schists) ($n = 76$), (b) quartzofeldspathic lithologies (sheared igneous rocks) ($n = 66$), and (c) intersection of S–C surfaces in S–C structures indicating top-to-the WNW (direction perpendicular to S–C crenulation axes is plotted) ($n = 49$). The median trend from two-dimensional statistical analysis is included in the stereograms.

the case for D2. The D2 folds, crenulations, and related intersection lineations show a relatively consistent regional northeast trend (Fossen 1993) except for local deviations in the southwestern part of the Bergsdalen Nappes east of the Major Bergen Arc (Fig. 17). This trend, which also has been reported from northwest Jotunheimen (cf. Milnes & Koestler 1985) and Hardangervidda (Andresen 1974) is at a high angle to the NW–SE trend of the D2 mineral and stretching lineations (Fig. 16). There is no indication that the D2 fold hinges rotated during deformation: open (Fig. 18a) and tight (Fig. 18b) folds all show the same range in orientation about NE–SE. Both the consistent asymmetry of the D2 kinematic indicators and independent strain considerations (Fossen 1992b) indicate that the bulk D2 deformation was strongly non-coaxial and close to simple shear. The décollement zone was subhorizontal at the onset of D2 (e.g. Milnes et al. 1988; Fossen 1992a), and it is assumed that the layering that formed and/or was transposed during thrusting was subparallel to the shear plane at the end of D1. During the D2 reverse movement, the subhorizontal F2 hinges must then have formed close to the shear plane. According to Figs. 11 and 13a, lines close to the shear plane do not rotate much for relatively small shear strains, which helps explain the apparently stable position of the F2 fold axes and intersection lineation during D2.

Discussion

It seems reasonable from the above discussion to assume that the trend (horizontal component) of the linear D1 fabric is parallel to, or at least close to, the nappe transport direction. The curvatures and changes in the linear D1 fabric pattern (Fig. 2) may thus reflect spatial and/or temporal variations in slip direction during thrusting (D1), and/or may be the result of reworking

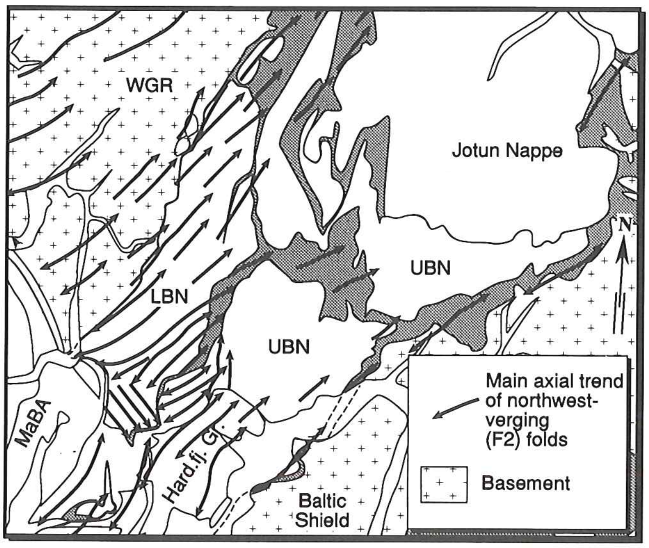

Fig. 17. Trend of F2 fold axes in the area covered by Fig. 1. See text for discussion.

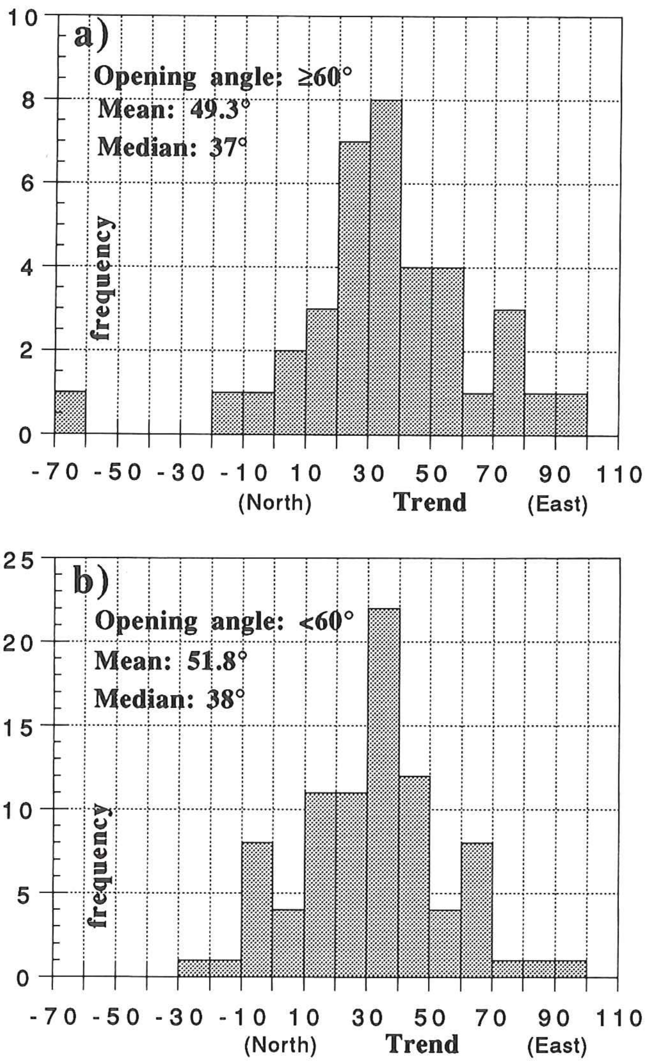

Fig. 18. Trend of D2 fold axes as separated into folds with opening angle (a) larger than and (b) smaller than 60°.

during the subsequent reverse movement (D2). Gentle, large-scale curvatures, as seen in the LBN and the southern part of the UBN, may be expressions of superposed D2 deformation. However, other changes in the linear fabric are more pronounced and abrupt, particularly between the northern part of the LBN and UBN, and between the WGR and the LBN. It is suggested, as a preliminary model, that these changes reflect different slip directions in different tectonic units during the thrusting history, where the basement (WGR) deformed by lateral shear, and the overriding Bergsdalen Nappes experienced orogen normal (transverse) thrusting (Fig. 19). Partitioning of deformation into orogen-parallel (strike-slip) and orogen-normal (thrusting) shear components appears to be common in the internal parts of orogens (e.g. Bryant & Reed 1969; Dewey et al. 1986; Ellis & Watkinson 1987; Oldow et al. 1990) and has recently been suggested as a model for the northeastern portion of the WGR (Gilotti & Hull 1991; Séranne 1992).

The constrictional strain recorded within the Bergsdalen Nappes, which in this paper is interpreted as the

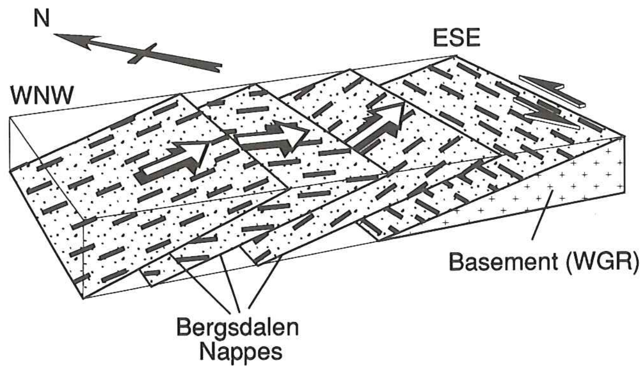

Fig. 19. Simplified model indicating different shear directions (arrows) and lineation trends (black lines) in the WGR and the Bergsdalen Nappes during thrusting (D1). Note that the figure illustrates the geometric situation during thrusting, when the Bergsdalen Nappes presumably were dipping gently to the WNW (cf. Fossen 1992b).

result of combined thrusting and horizontal pure shear, is harder to understand in a larger, tectonic context, and represents a general problem in many regions of penetrative ductile deformation. The shortening perpendicular to the thrusting direction must, however, have been compensated for by extension in the same direction in the surrounding units, most likely in the phyllites, which show a weaker L-fabric than the rocks of the Bergsdalen Nappes.

The more uniform and consistent trend of the linear structures related to the backward movement of the Jotun Nappe reflects a simpler deformation history during D2 than during D1, and suggests a uniform translation of the Jotun Nappe to the WNW. It is argued that the D2 lineation and the reversed movement is related to large-scale Lower to Middle Devonian extensional tectonics prior to the development of the Mid-Devonian basins to the NW of the study area (cf. Fossen 1992a).

Conclusions

Two sets of linear fabrics are found in the Bergsdalen Nappes and the surrounding phyllite/mica schist, and are interpreted as having formed during two temporally distinct events. The early set is pervasive throughout the region, comprising a variety of parallel stretching, mineral and intersection lineations, and thought to be the result of Caledonian thrusting (D1). The parallelism of F1 fold axes and other L1 linear structures is striking, and a combination of simple shear thrusting and horizontal pure shear with shortening perpendicular to the thrusting direction is favored as a general model since it provides a more efficient means of rotating fold axes parallel to the lineation and adequately explains the constrictional strains observed in the Bergsdalen Nappes.

The second set of stretching and fiber lineations (L2) is related to post-orogenic reversed movement of the Jotun Nappe and is associated with crustal extension. Their uniform trend of about 295° is interpreted to represent the direction of reverse movement. However, fold axes and related crenulation or intersection lineations form at a high angle to this direction. Since rotation of these folds during the reversed movement seems scarce or absent, they are interpreted as having formed in or close to the shear plane.

Acknowledgements. – The author is grateful to encouragement and help from T. B. Holst, P. J. Hudleston, and C. P. Teyssier during this project, and for reviews by A. G. Milnes and H. Sjøstrøm. T. Torske is thanked for taking the time to introduce the author to the geology along the northwestern side of Folgefonnshalvøyen. This work was supported by NAVF (grant No. 440.89/061). Additional support from Statoil and the University of Minnesota is acknowledged.

Manuscript received May 1992

References

Anderson, E. M. 1948: On lineation and petrofabric structure, and the shearing movement by which they have been produced. *Quartery Journal of the Geological Society of London 54,* 99–126.
Andresen, A. 1974: Petrographic and structural history of the Caledonian rocks north of Haukelisæter, Hardangervidda. *Norges geologiske undersøkelse 314,* 1–52.
Bell, T. H. 1978: Progressive deformation and reorientation of fold axes in a ductile mylonite zone: the Woodroffe thrust. *Tectonophysics 44,* 285–320.
Bryant, B. & Read, J. C. 1969: Significance of lineations and minor folds near major thrust faults in the southern Appalachians and the British and Norwegian Caledonides. *Geological Magazine 106,* 412–429.
Burg, J-P., Bale, P., Brun, J-P. & Girardeau, J. 1987: Stretching lineation and transport direction in the Ibero-Armorican arc during the Siluro-Devonian collision. *Geodinamica Acta 1,* 71–87.
Cloos, E. 1946: Lineation. *Geological Society of America Memoir 18,* 122 pp.
Cobbold, P. & Quinquis, H. 1980: Development of sheath folds in shear regimes. *Journal of Structural Geology 2,* 119–126.
Coward, M. P. & Potts, G. J. 1983: Complex strain patterns developed at frontal and lateral tips to shear zones and thrust zones. *Journal of Structural Geology 5,* 383–399.
Dennis, A. J. & Secor, D. T. 1990: On resolving shear direction in foliated rocks deformed by simple shear. *Geological Society of America Bulletin 102,* 1257–1267.
Dewey, J. F., Hempton, M. R., Kidd, W. S. F., Saroglu, F. & Sengör, A. M. 1986: Shortening of continental lithosphere: neotectonics of eastern Anatolia – a young collision zone. *In* Coward, M. P. & Ries, A. C. (eds.): Collision Tectonics. *Geological Society of London Special Publication 19,* 3–36.
Dons, J. A. 1960: Telemark supracrustals and associated rocks. *In* Holtedahl, O. (ed.): Geology of Norway. *Norges geologiske undersøkelse 208,* 49–58.
Ellis, M. & Watkinson, A. J. 1987: Orogen-parallel extension and oblique tectonics: the relation between stretching lineations and relative plate motions. *Geology 15,* 1022–1026.
Escher, A. & Watterson, J. 1974: Stretching fabrics, folds and crustal shortening. *Tectonophysics 22,* 223–231.
Flinn, D. 1962: On folding during three-dimensional progressive deformation. *Quarterly Journal of the Geological Society, London 118,* 385–433.
Flinn, D. 1979: The deformation matrix and the deformation ellipsoid. *Journal of Structural Geology 1,* 299–307.
Fossen, H. 1988: The Ulriken Gneiss Complex and the Rundemanen Formation: a basement–cover relationship in the Bergen Arcs, West Norway. *Norges geologiske undersøkelse 412,* 67–86.
Fossen, H. 1992a: The nature and significance of extensional tectonics in the Caledonides of South Norway. *Journal of Structural Geology 14,* 1033–1046.
Fossen, H. 1992b: Devonian extensional deformation in the Caledonian orogen, southern Norway. PhD thesis, University of Minnesota, 169 pp.
Fossen, H. 1993: Structural evolution of the Bergsdalen Nappes, Southwest Norway. *Norges geologiske undersøkelse,* in press.
Fossen, H. & Tikoff, B. 1993: The unified deformation matrix, and its applications in structural modelling. *Journal of Structural geology 15,* in press.
Gilotti, J. A. & Hull, J. M. 1991: A new tectonic model for the central Scandinavian Caledonides. *Terra Nova 3,* 18.
Gray, J. W. 1978: Structural history and Rb-Sr geochronology of Eksingedalen, west Norway. PhD thesis, University of Aberdeen, 218 pp.
Hammer, S. K. 1979: The role of heterogeneities and linear fabrics in the formation of crenulations. *Journal of Structural Geology 1,* 81–91.

Henderson, J. R. 1981: Structural analysis of sheath folds with horizontal X-axes, northeast Canada. *Journal of Structural Geology 3*, 203–210.
Hobbs, B. E., Means, W. D. & Williams, P. F. 1976: *An outline of Structural Geology*, 571 pp. Wiley, New York.
Holst, T. B. & Fossen, H. 1987: Strain distribution in a fold in the West Norwegian Caledonides. *Journal of Structural Geology 9*, 915–924.
Hossack, J. 1968: Pebble deformation and thrusting in the Bygdin area (Southern Norway). *Tectonophysics 5*, 315–339.
Hsu, T. C. 1966: The characteristics of coaxial and non-coaxial strain paths. *Journal of Strain Analysis 1*, 216–222.
Hudleston, P. J. 1977: Similar folds, recumbent folds and gravity in ice and rocks: *Journal of Geology 85*, 113–122.
Hudleston, P. J. 1989: The association of folds and veins in shear zones. *Journal of Structural Geology 11*, 949–958.
Kerrich, R. & Allison, I. 1978: Flow mechanisms in rocks. *Geoscience Canada 5*, 109–118.
Kirschner, D. & Teyssier, C. 1992: Deformation history of the White Range duplex, central Australia, with implications for fold reorientation. *Australian Journal of Earth Sciences 39*, 441–456.
Kvale, A. 1946: Petrologic and structural studies in the Bergsdalen quadrangle, western Norway, part I. Petrography. *Bergen Museums Årbok 1946–47, Naturvit. rekke 1.*
Kvale, A. 1948: Petrologic and structural studies in the Bergsdalen quadrangle, western Norway, part II. Structural geology. *Bergen Museums Årbok 1946–47, Naturvit. rekke 1*, pp. 1–255.
Kvale, A. 1953: Linear structures and their relation to movements in the Caledonides of Scandinavia and Scotland. *Quarternary Journal of the Geological Society 109*, 51–73.
Lacassin, R. and Mattauer, M. 1985: Kilometre-scale sheath fold at Mattmark and implications for transport direction in the Alps. *Nature 315*, 739–742.
Lin, S. & Williams, P. F. 1992: The geometrical relationship between the stretching lineation and the movement direction of shear zones. *Journal of Structural Geology 14*, 491–498.
Lindström, M. 1961: Beziehungen zwischen Kleinfaltungvergenzen und anderen Gefügemerkmalen in den Kaledoniden Skandinaviens. *Geologische Rundschau 51*, 144–180.
Lisle, J. 1984: Strain discontinuities within the Seve–Köli Nappe Complex, Scandinavian Caledonides. *Journal of Structural Geology 6*, 101–110.
March, A. 1932: Matematische Theorie der Regelung nach der Korngestalt bei affined Deformation. *Zeitschrift für Krystallographie 81*, 285–297.
Mattauer, M., Faure, M. & Malavielle, J. 1981: Transverse lineation and large-scale structures related to Alpine obduction in Corsica. *Journal of Structural Geology 36*, 6401–6409.
McLelland, J. M. 1984: The origin of ribbon lineation within the southern Adirondacks, U.S.A. *Journal of Structural Geology 6*, 147–157.
Means, W. D., Hobbs, B. E., Lister, B. E. & Williams, P. F. 1980: Vorticity and non-coaxiality in progressive deformations. *Journal of Structural Geology 2*, 371–378.
Milnes, A. G., Dietler, T. N. & Koestler, A. G. 1988: The Sognefjord northshore log – a 25 km depth section through Caledonized basement in western Norway. *Norges Geologiske Undersøkelse Special Publication 3*, 114–121.
Milnes, A. G. & Koestler, A. G. 1985: Geological structure of Jotunheimen, southern Norway (Sognefjell-Valdres cross-section). *In* Gee, D. G. & Sturt, B. A. (eds.): *The Caledonide Orogen – Scandinavia and Related Areas*, 457–474. Wiley, New York.
Oldow, J. S., Bally, A. W. and Lallemant, G. A. 1990: Transpression, orogenic float, and lithospheric balance. *Geology 18*, 991–994.
Pringle, I. R., Kvale, A. & Anonsen, L. B. 1975: The age of the Hernes granite, Lower Bergsdalen Nappe, western Norway. *Norsk Geologisk Tidsskrift 55*, 191–195.
Ramsay, J. G. & Graham, R. H. 1970: Strain variation in shear belts. *Canadian Journal of Earth Sciences 7*, 786–813.
Rhodes, S. & Gayer, R. A. 1977: Non-cylindrical folds, linear structures in the x-direction and mylonite developed during translation of the Caledonian Kalak Nappe Complex of Finmark. *Geological Magazine 114*, 329–341.
Ridley, J. 1986: Parallel stretching lineations and fold axes oblique to a shear displacement direction – a model and observations. *Journal of Structural Geology 8*, 647–653.
Roberts, J. L. & Sanderson, D. J. 1973: Oblique fold axes in the Dalradian rocks of the southwest Highlands. *Scottish Journal of Geology 9*, 281–296.
Robin, P-Y. 1979: Theory of metamorphic segregation and related processes. *Geochimica et Cosmochimica Acta 43*, 1587–1600.
Sander, B. 1930: *Gefügekunde der Gesteine*, 352 pp. Springer, Vienna.
Sanderson, D. J. 1973: The development of fold axes oblique to the regional trend. *Tectonophysics 15*, 55–70.
Séranne, M. 1992: Late-Paleozoic kinematics of the Møre–Trøndelag fault zone and adjacent areas, central Norway. *Norsk Geologisk Tidsskrift 72*, 141–158.
Shedl, S. & van der Pluijm, B. A. 1988: A review of deformation microstructures. *Journal of Geological Education 36*, 111–121.
Skjernaa, L. 1980: Rotation and deformation of randomly oriented planar and linear structures in progressive simple shear. *Journal of Structural Geology 2*, 101–109.
Treagus, J. E. & Treagus, S. H. 1981: Folds and the strain ellipsoid: a general model. *Journal of Structural Geology 3*, 1–17.
Vernon, R. H. 1974: Controls on mylonitic compositional layering during non-cataclastic ductile deformation. *Geological Magazine 111*, 121–123.
Vollmer, F. W. 1988: A computer model of sheath-nappes formed during crustal shear in the Western Gneiss Region, central Norwegian Caledonides. *Journal of Structural Geology 10*, 735–745.
Williams, G. D. 1978: Rotation of contemporary folds into the X direction during overthrust processes in Laksefjord, Finnmark. *Tectonophysics 48*, 29–40.
Wilson, C. J. L. 1975: Preferred orientation of quartz ribbon mylonites. *Geological Society of America Bulletin 86*, 968–974.

Appendix

The random distribution of fold axes (lines) that were deformed as shown in Fig. 11 was generated in the following way. A random-number generator was used to generate numbers between 0 and 360 for the trend of the lines, together with a random number between 0 and 1, which is the cosine of the angle ϕ between the line and the z-axis (i.e. the third component of the unit vector parallel with the line). The plunge of a random line is then simply 90-arccos(ϕ). The lines were deformed using the deformation matrices (**D**)

$$\underset{\text{THRUST}}{\begin{pmatrix} 1 & 0 & \gamma_T \\ 0 & 1 & 0 \\ 0 & 0 & 1 \end{pmatrix}} \qquad \underset{\text{THRUST + WRENCH}}{\begin{pmatrix} 1 & \gamma_W & \gamma_T \\ 0 & 1 & 0 \\ 0 & 0 & 1 \end{pmatrix}} \qquad \underset{\text{THRUST + PURE SHEAR}}{\begin{pmatrix} k & 0 & \dfrac{\gamma_T(k-1)}{\ln k} \\ 0 & k^{-1} & 0 \\ 0 & 0 & 1 \end{pmatrix}}$$

where γ_T = thrust component, γ_W = wrench component, and k = the extension (pure shear) factor in the shearing or X-direction (cf. Fossen & Tikoff 1993). The new line vector l' is found by the relationship $l' = \mathbf{D}l$ where l is the unit vector parallel with the undeformed line, and l' is the new vector after deformation (cf. Flinn 1979).